Journal of Materials Chemistry A

Accepted Manuscript

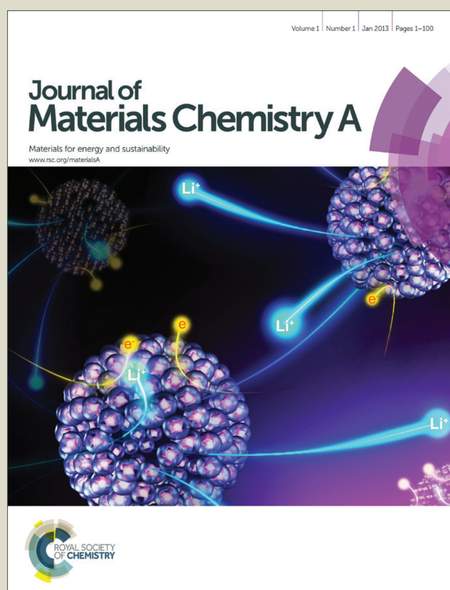

This is an *Accepted Manuscript*, which has been through the Royal Society of Chemistry peer review process and has been accepted for publication.

Accepted Manuscripts are published online shortly after acceptance, before technical editing, formatting and proof reading. Using this free service, authors can make their results available to the community, in citable form, before we publish the edited article. We will replace this *Accepted Manuscript* with the edited and formatted *Advance Article* as soon as it is available.

You can find more information about *Accepted Manuscripts* in the Information for Authors.

Please note that technical editing may introduce minor changes to the text and/or graphics, which may alter content. The journal's standard Terms & Conditions and the Ethical guidelines still apply. In no event shall the Royal Society of Chemistry be held responsible for any errors or omissions in this *Accepted Manuscript* or any consequences arising from the use of any information it contains.

ROYAL SOCIETY OF CHEMISTRY

www.rsc.org/materialsA

Table of contents entry

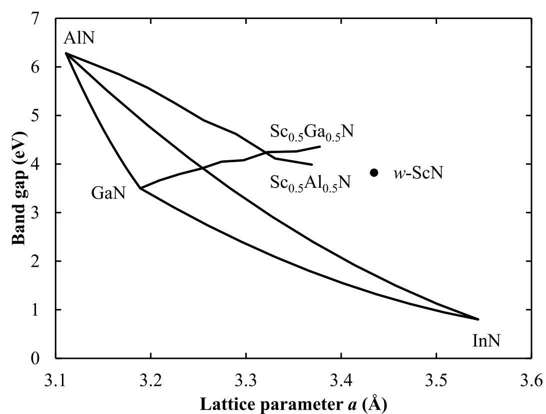

ScAlN and ScGaN alloys are wide band-gap semiconductors which can greatly expand the options for band gap and polarisation engineering required for efficient III-nitride optoelectronic devices, high-electron mobility transistors and energy-harvesting devices.

Journal of Materials Chemistry A Accepted Manuscript

Journal Name RSCPublishing

ARTICLE

ScGaN and ScAlN: emerging nitride materials

Cite this: DOI: 10.1039/x0xx00000x

M.A. Moram[a] and S. Zhang[b]

Received 00th January 2012,
Accepted 00th January 2012

DOI: 10.1039/x0xx00000x

www.rsc.org/

This review addresses the recent development and future prospects for Sc-based III-nitride alloys in energy-efficient device applications. Wurtzite-structure ScAlN and ScGaN alloys are wide band-gap semiconductors which can be stabilised at the low Sc contents relevant to devices, can be grown epitaxially, include the lattice-matched $Sc_{0.18}Al_{0.82}N$/GaN system, retain direct band gaps in the near-UV region up to 25% ScN and 50% ScN respectively, and should offer significantly higher exciton binding energies and piezoelectric coefficients compared to other III-nitrides. These properties greatly expand the options for band gap and polarisation engineering required for efficient optoelectronic devices, high-electron mobility transistors and energy-harvesting devices.

Introduction

Motivations for developing Sc-based nitrides

The conventional wurtzite-structure group-III nitride materials InN, GaN and AlN are currently used widely in energy applications. For example, InGaN-based blue and green light emitting diodes (LEDs) have enabled energy-efficient solid-state lighting [1, 2], while AlGaN-based ultraviolet LEDs are of emerging interest for energy-efficient water treatment applications [3]. Recently, AlGaN- and InAlN-based high electron mobility transistors have become important for energy-efficient power electronics [4]. Furthermore, AlN and related nitride materials perform very well in energy harvesting devices, RF devices and in lead-free, high-temperature, piezoelectric applications [5]. The III-nitrides are also of growing interest as thermoelectric materials [6, 7].

However, the restricted range of III-nitride material properties limits the performance of these devices. For example, the internal quantum efficiency of III-nitride-based LEDs and lasers is limited by the quantum-confined Stark effect (QCSE), which produces a spatial separation of electron and hole wavefunctions within the light-emitting quantum well region of the device [8, 9]. This effect occurs due to a mismatch in the internal polarisation of the different III-nitride materials at interfaces in epitaxial heterostructures. The QCSE can be reduced using alternative 'non-polar' and 'semi-polar' thin film crystallographic orientations, or by using device designs which produce improved electron-hole wavefunction overlap [10, 11]. This effect is also associated with a reduction in internal quantum efficiency with increasing operating current ('efficiency droop'): considerable research effort is currently under way to counteract efficiency droop through optimisation of device design [12, 13, 14].

In practice though, it is difficult to tune the internal polarisation of the materials widely enough to compensate for this effect because either the band gaps or the lattice constants become unsuitable when the composition of either layer in a heterostructure is changed. In-plane lattice mismatches lead to interfacial strain and ultimately the formation of misfit dislocations at heterointerfaces. Dislocation densities can be reduced using nanopatterned substrates [15, 16] and interlayers [17], but still remain significantly higher than in devices based on other semiconductors (e.g. GaAs). These dislocations reduce device efficiencies, reliabilities and lifetimes [18, 19, 20, 21] and are associated with poor efficiencies in the green and ultraviolet spectral regions [1, 3]. Similarly, the performance of AlN and related materials in energy harvesting applications is limited by its relatively low piezoelectric coefficients [5]. These issues have motivated the search for additional tetrahedrally-bonded nitride materials which might offer additional degrees of freedom for tuning the piezoelectric coefficients and which could offer wider options for lattice- and polarisation-matching in device heterostructures. We propose that these goals could be realised using an additional family of wurtzite-structure III-nitride materials based on Sc.

Why scandium?

The properties of the Group III nitrides could be extended most straightforwardly by replacing either the Group III cation or the Group V anion. However, P has a very low solubility in GaN [22] and the solubility of the remaining Group V elements is even lower. Similarly, the remaining Group III elements B and Tl have low solubilities in GaN and AlN and there are further

Journal of Materials Chemistry A Accepted Manuscript

This journal is © The Royal Society of Chemistry 2013

concerns regarding the toxicity and poor volatility of Tl-based metalorganic precursors.

Alternatively, transition metals with an oxidation state of +3 could replace the Group III elements. Alloys between transition metal nitrides (TMNs) and the semiconducting Group III nitrides AlN and GaN are already known. Rock-salt structure TMNs themselves are of interest as thermoelectric materials [23, 24, 25, 26], while rock-salt structure TMN-AlN alloys are used extensively in hard coatings [27]. Dilute wurtzite-structure TMN-AlN and TMN-GaN alloys have also been investigated as magnetic semiconductors [28]. The stability of these alloys is known to depend on the size mismatch between the transition metal and the Group III element and on electronic effects [27]. Research efforts have concentrated on transition metals from the first row of the *d*-block in the Periodic Table, as these have the smallest atomic size mismatch with Al and Ga. Although bonding in TM-AlN alloys is complex, some general trends can be identified. At dopant concentrations, the TMs introduce localised states within the band gap [29], while at higher concentrations the conduction band in the resulting wurtzite-structure TMN-AlN alloys becomes dominated by partly-filled TM 3*d* states and hence the Fermi level lies inside the conduction band [29, 30]. This leads to metallic properties and to reduced phase stability (due to occupation of anti-bonding states). It is difficult to accurately determine TMN solubilities in III-nitrides due to the experimental difficulty of detecting the onset of formation of secondary phases, but solubility limits in GaN and AlN are known to be quite low, ranging from 0.4% for FeN in GaN [31] to around 4% for MnN in GaN [28, 32] and even lower in general for TMNs in AlN [33, 34, 35, 36].

Unlike the other 4th row transition metals, Sc in its usual +3 oxidation state has empty 3*d* orbitals, so its chemical behaviour is between that of transition metals and Group III elements [37]. For example, although ScN has the same rock-salt crystal structure and a very similar band structure compared to other TMNs [38], Sc has fewer valence electrons and so the Fermi level in ScN drops below the conduction band edge, leading to semiconducting behaviour instead of the metallic properties of other rock-salt TMNs. Indeed, both theory [39, 40] and experiment [41, 42] show clearly that ScN is a semiconductor with a fundamental indirect gap of 0.9 eV and a direct gap of 2.1 eV, which can be incorporated directly into III-nitride structures [43] and which can be grown successfully using a wide range of techniques [44, 45, 46, 47, 48, 49, 50, 51] (although its band gap can be affected quite strongly by oxygen incorporation: at low oxygen contents this most likely occurs via a Moss-Burnstein shift [24, 25, 42]).

This review will now discuss the unique properties of Sc-based III-nitrides which arise from choosing semiconducting ScN instead of metallic TMNs as an alloy end member. The focus is on wurtzite-structure ScGaN and ScAlN, as these alloys are expected to have relatively wide band gaps (of interest for optoelectronics and high power devices) and as they are expected to be reasonably easy to create experimentally by molecular beam epitaxy (unlike ScInN), as there are only moderate differences in the vapour pressures of the constituent metals.

Unique properties of ScGaN and ScAlN alloys

Phase stability

A useful parameter in these binary alloy systems is the TMN concentration at which the least unstable alloy phase is predicted to transition from wurtzite to rock-salt. This concentration is usually much higher than the real TMN solubility limit in wurtzite GaN or AlN, but is a useful guide for comparison with other TMN-III-nitride alloys. Fig. 1 shows that ScAlN prefers a hexagonal structure up to 56% ScN and ScGaN prefers a hexagonal structure up to 66% ScN [52]†. The data for ScAlN are consistent with previous studies focusing on the phase stability of cubic and hexagonal ScAlN alloys [61].

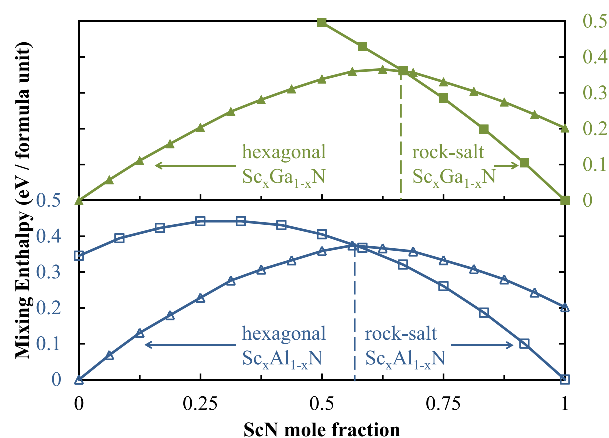

Fig. 1. Mixing enthalpies for different ScGaN and ScAlN phases across the full alloy composition range (from [52]).

ScGaN and ScAlN behave similarly, as expected given the small lattice parameter difference of about 2% between AlN and GaN. However, in both cases the wurtzite phase remains stable up to a significantly higher TMN content than in other TMN-AlN and TMN-GaN alloys. Using a similar calculation method, the wurtzite to rock-salt transition was predicted to occur at lower TMN contents, for example around 31% TiN in TiAlN [53], 33% CrN in CrAlN [54] and 30% NbN in NbAlN [29]. This is consistent with the recent prediction that ScN, when introduced as an impurity into AlN, produces the least stabilisation of the rock-salt phase of the 4th-row TMNs†† [27].

The greater relative stability of the wurtzite phase in ScAlN and ScGaN appears to be due to electronic effects. Considering size effects alone, Sc in the +3 state has a greater ionic radius than any other 4th row transition metal in the +3 state and so we might expect ScAlN to be less stable than other TMN-AlN alloys. However, electronic effects associated with the empty Sc 3*d* orbitals are significant. To illustrate, we can compare results for wurtzite-structure ScAlN [52] and NbAlN [29]

Journal of Materials Chemistry A Accepted Manuscript

 This journal is © The Royal Society of Chemistry 2012

calculated using a similar approach. In ScAlN, the Sc 3*d* orbitals contributing to the conduction band are empty and the Fermi level lies in the gap. There is minimal energetic stabilisation to be gained by bringing the Sc 3*d* states into bonding (even at room temperature where some carriers will be present in the conduction band), so sp^3 hybridisation should be retained locally at the Sc atoms. In contrast, the Nb 3*d* states contributing to the conduction band are partly occupied and therefore the Fermi level lies inside the conduction band. The overall energy of the system is then reduced by bringing partly-filled Nb 3*d* states into bonding via a trend towards localised sp^3d orbital hybridisation at the Nb atoms. Consistent with these findings, only a minor local structural distortion away from wurtzite-like tetrahedral bonding is predicted [52, 55] and observed in dilute ScGaN, whereas the local bonding around Nb in NbAlN tends more strongly towards 5-fold coordination [29]. This structural distortion, along with the high density of states at the Fermi level (useful as a relative guide to phase stability [30]), inherently destabilises the wurtzite phase in NbAlN. A corresponding effect cannot occur in rock-salt TMN-AlN alloys in which sp^3d^2 hybridisation in involved and large distortions from octahedral coordination are impossible. Consequently, a greater relative stabilisation of the wurtzite phase is expected for ScAlN than for NbAlN or other TMN-AlN alloys at equivalent TMN concentrations.

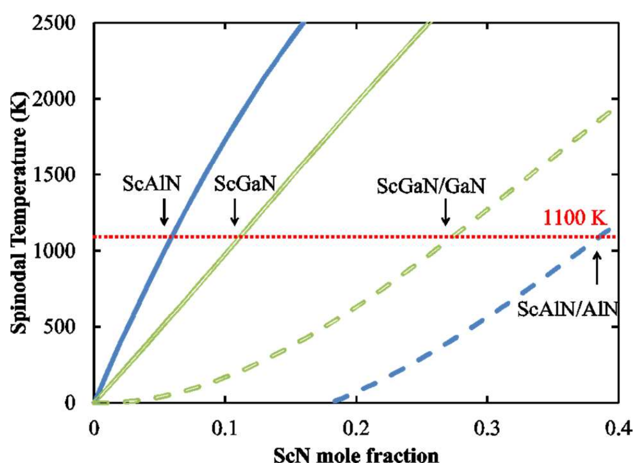

Fig. 2. Predicted compositional regions in which unstrained ScGaN and ScAlN and strained ScGaN on GaN and ScAlN on GaN (or AlN) should be stable with respect to spinodal decomposition at around 825 °C (from [52]).

A more accurate but less frequently calculated measure of phase stability is the TMN concentration at which the wurtzite-structure TMN-AlN alloy is stable with respect to spinodal decomposition into Sc-rich rock-salt and Sc-poor wurtzite phases. This concentration is usually far lower than that of the wurtzite to rock-salt phase transition. The corresponding values predicted for *unstrained* ScAlN and ScGaN are 6% ScN and 11% ScN respectively at typical thin film growth temperatures of around 825 °C (Fig. 2). Although relatively low, these values are greater than other TMN-AlN alloys (e.g. TiAlN should contain less than ~2% Ti to remain stable against spinodal decomposition at 900 °C [56]) and are closer to unstrained InGaN, which is used widely in devices [57].

Some experimental data exists for comparison with these predictions. Most experimental reports describe columnar ScAlN films with relatively high ScN contents deposited by magnetron sputtering, a technique which operates far from equilibrium and where growth temperatures [58] and substrate effects are known to influence phase stabilities [59]. Sputtered single-phase wurtzite ScAlN films have been confirmed for compositions below 20% ScN [60], 22% ScN [61] below 30% ScN [59, 62] and below 43% ScN [58] depending on growth conditions. Lower growth temperatures tend to preserve single-phase material [58, 63]. Mixed phase and purely rock-salt ScAlN films are reported for higher ScN contents [59, 61, 62, 64]. Other growth methods have been attempted, although there may be some difficulty with incorporating Sc into AlN [65, 66].

Single-phase wurtzite-structure ScGaN films have also been reported for ScN contents < 17%, but mixed-phase and rock-salt films are found at higher ScN contents [67, 68] while one report indicates only nanocrystalline material across the whole composition range [69]. This situation is similar to other TMN-AlN alloys, in which mixed phase films are deposited frequently and in which reports of the wurtzite - rock salt phase transition vary widely [29]. Mixed phases appear to occur due to the statistical variations in local composition expected for random alloys, combined with the sensitivity of the wurtzite-rock salt phase transition point to the effects of growth temperature, stresses and crystal defects [53, 54, 70]. Decomposition of films with average compositions outside the spinode but inside the binode may also occur via the nucleation and growth of precipitates, although this process is usually kinetically inhibited.

Reasonably low defect density epitaxial ScGaN films approaching device quality have also been reported [71, 72]. In-plane epitaxial strain is predicted to influence the onset of spinodal decomposition greatly and should increase the phase-stable composition range for *compressively strained* ScAlN on GaN (or on AlN) to ≈ 40% ScN and ScGaN on GaN up to ≈ 27% ScN (Fig. 2). In fact, the epitaxial strain enhancement of the phase stability of InGaN films on GaN is essential for achieving single-phase layers in practice [73, 74]. Consequently, epitaxially strained ScAlN and ScGaN films suitable for use in semiconductor devices should show much better phase stability than sputtered films. However, for ScAlN and ScGaN films with higher ScN contents, there is some indication that decomposition may proceed via nucleation and growth, even at compositions where spinodal decomposition is thermodynamically favoured [75].

Journal of Materials Chemistry A Accepted Manuscript

Lattice parameters, electronic structure and band gaps

	$Sc_xAl_{1-x}N$			$Sc_xGa_{1-x}N$		
x	*a*	*c*	Cor. *a*	*a*	*c*	Cor. *a*
0	3.125	5.010	3.111	3.244	5.276	3.189
0.0625	3.152	5.025	3.138	3.262	5.286	3.209
0.125	3.180	5.037	3.166	3.280	5.292	3.230
0.1875	3.211	5.037	3.197	3.300	5.290	3.253
0.25	3.239	5.049	3.225	3.319	5.295	3.274
0.3125	3.270	5.049	3.256	3.340	5.293	3.297
0.375	3.303	5.032	3.289	3.362	5.278	3.323

Table 1. The a and c lattice parameters of wurtzite ScGaN and ScAlN around the phase-stable compositional region, from [52] and consistent with [64], including in-plane lattice parameters corrected with respect to experimental data ('Cor. a'). All lattice parameter values given in Å.

This section now focuses on the hexagonal phases of interest for electronic device applications. It is important to note that the *c/a* lattice parameter ratio can vary from ≈ 1.6 to 1.2 and the internal parameter *u* can vary from ≈ 0.38 to 0.5 within the wurtzite structure. At the furthest end of this range (*c/a* = 1.2 and *u* = 0.5) the wurtzite structure changes into a flattened, 5-fold coordinated nonpolar 'B_k' phase (*P63/mmc*). For pure ScN, this nonpolar phase is calculated to be the most stable of the possible hexagonal phases [76, 77, 78] whereas wurtzite ScN with the 'ideal' *c/a* ratio of ~1.6 is entirely unstable [76]. Consequently, a reduction in the *c/a* ratio and an increase in *u* is expected to occur with increasing ScN content for both ScAlN and ScGaN, as the structure moves from undistorted wurtzite (i.e. the stable phase of GaN and AlN) towards the related hexagonal B_k phase (i.e. the metastable phase of ScN). This means that to accurately predict lattice parameters, it is essential to relax the *c/a* ratio and *u* parameter of the simulation supercells. As expected, a gradual decrease in the *c/a* ratio and an increase in *u* is predicted [52], consistent with experimental observations for sputtered ScAlN [50, 51] and for ScGaN [67, 68, 71, 72]. Predicted ScGaN and ScAlN lattice parameters are given in Table 3; additional in-plane values are also given which have been corrected with respect to experimental data for GaN and AlN in order to better predict the true experimental values.

The electronic structures of ScGaN and ScAlN derived from correctly relaxed supercells can now be discussed. The wurtzite structure is expected to be preferred for ScGaN up to approximately 66% ScN and for ScAlN up to approximately 56% ScN. Over these composition ranges, it is clear that both alloys remain semiconducting, but there are significant differences in the densities of states in their conduction bands [52] (Fig. 4). The conduction band edge of ScAlN is dominated by localised Sc 3*d* states at all ScN contents, leading to a flattened band dispersion around the Γ point. In contrast, the conduction band edge of ScGaN is dominated by Ga states. This occurs because the Sc 3*d* states are at relatively similar energies with respect to the valence band maximum in both alloys, but in dilute ScAlN the Al states lie above the Sc 3*d* states whereas in dilute ScGaN the Ga states lie below the Sc 3*d* states (as expected, given that the band gap of AlN is almost twice as large as that of GaN).

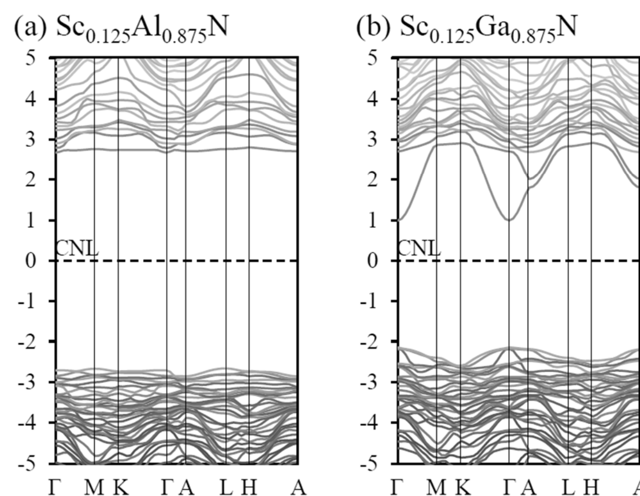

Fig. 3. Calculated electronic structures of (a) ScAlN and (b) ScGaN with a ScN content of 12.5% (from [52]).

For ScGaN, trends in from X-ray absorption near-edge spectroscopy (XANES) data suggest that bonding in ScGaN becomes more ionic as the Sc content increases, as predicted [79]. XANES data also suggest a small local structural distortion at the Sc atoms [45], as predicted and investigated previously [52, 67, 68]. However, in contrast to other TMN-III-nitride alloys [29], such distortions should have only minor effects on the ScGaN band structure [52].

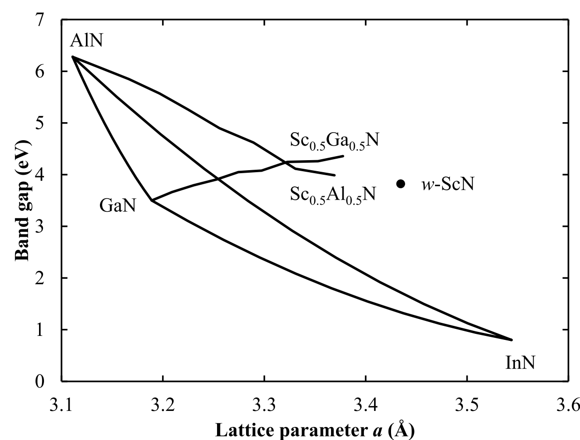

Fig. 4. Corrected band gap vs. in-plane lattice parameter plot for unstrained ScGaN and ScAlN. Data are derived from calculations and corrections in [52] and are consistent with experimental reports [60, 64].

The alloy band gaps can then be predicted, based on results from optimised electronic structure calculations. Although it is difficult to predict absolute band gap values correctly using density functional theory, the relative trends calculated for a series of alloys should be reliable and the choice of suitable

Journal of Materials Chemistry A Accepted Manuscript

This journal is © The Royal Society of Chemistry 2012

band gap corrections enables realistic predictions to be made (Fig. 5) [52]. For ScAlN, a *decrease* in band gap with increasing ScN content is both predicted [52] and observed experimentally [60]. The band gaps of ScAlN are expected to stay direct up to approximately 25% ScN [52]. However, using the same calculation method and using lattice parameters consistent with experiment, an *increase* in band gap with increasing ScN content is predicted for ScGaN [52] (Fig. 4). The band gaps of ScGaN are expected to stay direct up to approximately 50% ScN. This result is consistent with the limited experimental data for high-quality epitaxial films [52]. It is reasonable to expect that calculations producing the correct (experimentally verified [64, 67, 68]) crystal structure for ScGaN and ScAlN and the correct (experimentally verified [60]) band gap trend for ScAlN should also predict correctly the band gap trend for ScGaN. However, the predicted trend for ScGaN differs from previous reports.

Previous theoretical predictions of the ScGaN band gap were based on supercells with significant short range ordering of Sc atoms (as well as using the wrong GaN band gap) which leads to the opposite trend, i.e. an increase in band gap with increasing lattice parameter [80]. Additionally, one experimental report describes a general decrease of the band gap with increasing ScN content [69], but reports highly inaccurate values for the band gaps of GaN: most of the data was obtained from nanostructured ScGaN films where phase separation almost certainly occurred. However, better-quality wurtzite-like ScGaN films appear to have band gaps that decrease slightly with increasing ScN content, at least up to ~17% ScN [67]. Here, we note that some downward band gap bowing invariably occurs in wide band gap alloys with a large lattice mismatch between the end members [81, 82], but is not predicted adequately from the relatively small simulation supercells used in density functional theory calculations. The results of Ref. 67 could therefore be consistent with an overall increase in band gap energies with increasing ScN content, on which there is superimposed a moderate downward band gap bowing, as expected for mismatched alloys. Additionally, a shallow defect band arising from the high density of planar defects (perhaps including some nanoscale zinc-blende regions) in the films of Ref. 67 is likely to have contributed to absorption below the conduction band edge.

The influence of other factors on the band gaps can also be assessed. Compressive in-plane strains are predicted to affect the magnitude of the band gaps of ScGaN and ScAlN, but the magnitude is only around ≈ 0.1 eV for low ScN contents, which is not enough to alter the band gap trends [52] (although a much greater effect is expected near the wurtzite to rock-salt phase transition). Impurities and/or nitrogen vacancies might affect measured band gaps through alloying effects or through changes in the carrier concentration leading to a Moss-Burnstein shift. Indeed, 2 at.% oxygen and around 0.1 at.% C and H were found to be incorporated in sputtered ScAlN films [61]. However, the calculated Moss-Burnstein shift decreases from 0.18 eV for AlN to 0.01 eV for ScAlN with 12.5% ScN and from 0.23 for GaN to 0.03 for ScGaN with 12.5% ScN (derived from [52]). This effect occurs due to the increasing density of Sc 3*d* states near the conduction band edge and so such shifts are not expected to be significant experimentally (band gap renormalisation effects are not expected to contribute strongly for similar reasons).

Additional parameters relevant to devices can be extracted from the band structure calculations, including the effective masses of electrons and holes. The valence band dispersion is quite flat in both alloys, indicating relatively high effective masses and low mobilities for holes. Exciton binding energies should also be significantly larger for both materials, potentially reaching as high as 240 meV for ScGaN with 37.5% ScN (value derived from Ref. [52] assuming a simple hydrogenic model and using dielectric constant data from Ref. [63]). For ScAlN, the Sc 3*d* states dominate the conduction band edge and therefore electrons are also expected to have high effective masses and relatively low mobilities. Polaronic conduction may therefore dominate in this material. However, because the Ga states dominate the conduction band edge in ScGaN, the theoretical results predict that electrons should retain effective masses and mobilities similar to those in GaN. Consequently, ScGaN and ScAlGaN alloys may find applications in the active regions of (opto)electronic devices where high carrier mobilities are required.

Elastic constants and piezoelectric properties

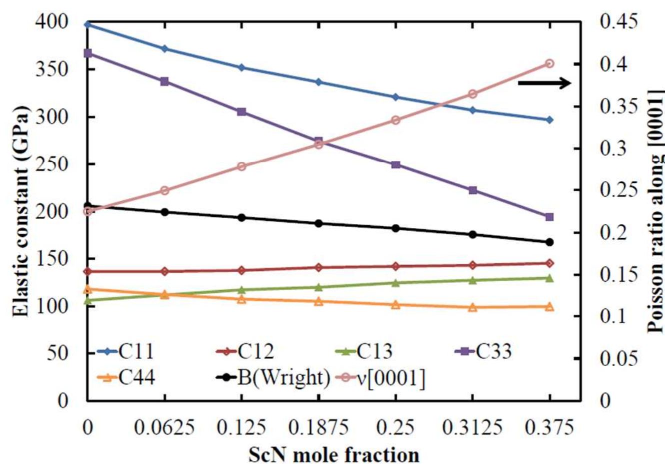

Fig. 5. Elastic constants of wurtzite-structure ScAlN; the elastic constants of ScGaN are similar (from [79]).

While the calculation and measurement of elastic constants are of great interest for cubic TMN-AlN alloys [83, 84], little attention has been paid to the elastic constants of the wurtzite TMN-AlN phases. However, the elastic constants are essential for use in device design and for composition determination using X-ray diffraction [85]. Recently, the elastic constants of both wurtzite-structure ScGaN and ScAlN were calculated: C_{11}, C_{33}, C_{44} and C_{66} were found to decrease while C_{12} and C_{13} increased

Journal of Materials Chemistry A Accepted Manuscript

slightly with increasing ScN contents [79]. The biaxial [0001] Poisson ratios also increased with increasing ScN content from 0.21 for GaN to 0.38 for $Sc_{0.375}Ga_{0.625}N$ and from 0.22 for AlN to 0.40 for $Sc_{0.375}Al_{0.625}N$, due to the increasing *u* values, in-plane bond lengths and average bond ionicities with increasing ScN contents [79]. These results are consistent with the softening previously predicted for ScAlN alloys with increasing ScN contents [86].

The piezoelectric performance of ScAlN and related alloys has also been of great interest recently, since high piezoelectric coefficients relative to AlN were predicted [86] and measured [58, 62, 64, 87]. Conveniently, the increase in piezoelectric coefficients is not accompanied by a substantial increase in dielectric constants. This leads to increased electromechanical coupling coefficients compared to AlN, as required for greater bandwidths in acoustic resonators [5, 63, 88] and for efficient performance in piezoelectric energy harvesters and related devices [88, 89].

The piezoelectric coefficient enhancement occurs because *u* can be increased more easily with an applied electric field due to the shallower and broader local ionic potential wells that develop when Sc is incorporated onto the metal sites [86]. The piezoelectric coefficients of ScGaN should be of a similar order to those of ScAlN. Importantly, the use of epitaxially strained or lattice-matched ScAlN/GaN or ScGaN/GaN heterostructures should lead to high 2D electron gas concentrations in HEMTs, due to the increased piezoelectric coefficients. Alternatively, opportunities for strain engineering may allow appropriate matching of the interfacial polarisations in quantum well structures used in optoelectronics.

Epitaxial growth and crystal defects in ScAlN and ScGaN

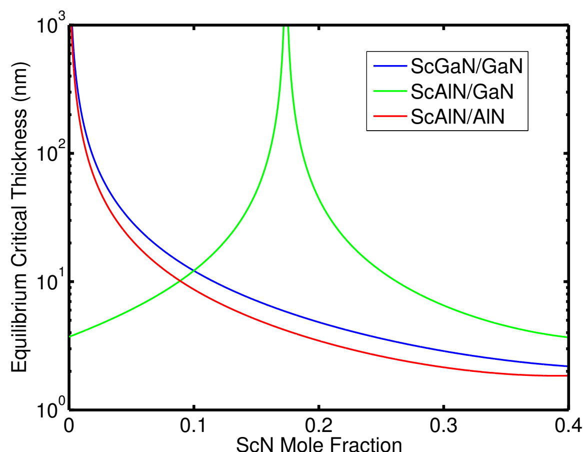

Fig. 6. Critical thicknesses for strain relaxation by dislocation glide for ScGaN/GaN, ScAlN/GaN and ScAlN/AlN [79].

In practice, it is essential to create epitaxial films with low defect densities for use in devices. The first criterion for successful growth of a lattice-mismatched epitaxial system is to prevent the introduction of defects due to strain relaxation in the epilayers. The prediction of critical thicknesses for strain relaxation in heterostructures including the conventional III-nitrides GaN and AlN is a very useful guide to this behaviour and has been completed for ScGaN on GaN, ScAlN on GaN and ScAlN on AlN [79]. Calculated critical thicknesses for relaxation by dislocation glide on the $^1/_3\langle 11\bar{2}3\rangle\{1\bar{1}01\}$ slip system range from 2 nm for ScAlN/AlN and ScGaN/GaN with 37% ScN to infinity for lattice-matched ScAlN/GaN with 18% ScN.

The second criterion is the possibility for epitaxial growth of low defect density films. Although no device-quality ScAlN films have yet been grown, high–quality epitaxial ScGaN films have already been achieved on GaN using molecular beam epitaxy with NH_3 as a nitrogen source [71, 72]. However, I_1-type basal plane stacking faults are observed in these films, in addition to a low density of nanoscale lamellar zinc-blende inclusions.

The basal plane stacking fault energies were not predicted to vary significantly with increasing Sc content in ScGaN [68], yet they are clearly observed in and epitaxial ScGaN films grown by two different methods [68, 70]. In contrast, no planar defects are visible in high-resolution micrographs of sputtered wurtzite-structure ScAlN films and there is no characteristic 'streaking' in the electron diffraction patterns either [61]. In Ref. 58 the presence of stacking faults in ScGaN was associated with the increasing local distortion (i.e. greater local *u*) at the Sc atoms. However, this local distortion is slightly greater in ScAlN compared to ScGaN [52], but no stacking faults or zinc blende inclusions have been observed in ScAlN films. Instead, we attribute this difference in behaviour to the different relative stability of the zinc-blende phases for each alloy. In GaN, the AαBβCγAαBβCγ-stacked zinc-blende phase is just 0.015 eV per formula unit higher in energy than the AαBβAαBβ-stacked wurtzite phase, meaning that faults in the *hcp* stacking sequence may form with relative ease. Indeed, zinc-blende GaN films can be grown using MBE under non-equilibrium conditions. In contrast, for AlN, the zinc blende phase is 0.043 eV per formula unit higher in energy than the wurtzite phase, so the relative probability of forming a faulted stacking sequence or inclusions of the metastable zinc blende phase is much lower in ScAlN.

Nanoscale lamellar inclusions of the zinc-blende phase are also found in epitaxial ScGaN films with ScN concentrations below the predicted onset for spinodal decomposition [79]. Although decomposition via nucleation and growth might occur, this should generate a Sc-poor wurtzite phase and a Sc-rich rock-salt phase. It could be argued that the phase stability of precipitates or inclusions is affected by the interfacial energies between phases, especially in the case of nucleation and growth [90], and this factor is not included in calculations. However, the zinc blende phase of ScN is highly unstable with respect to the rock-salt phase [91] and accordingly the zinc blende inclusions do not appear to be Sc-enriched. As for the case of

Journal of Materials Chemistry A Accepted Manuscript

This journal is © The Royal Society of Chemistry 2012

stacking faults, the zinc blende phase of GaN is only slightly metastable with respect to the wurtzite phase and ScGaN is expected to behave similarly to GaN at lower ScN contents. Consequently, these precipitates are not attributed to phase decomposition but to the appearance of a metastable zinc blende phase having a similar composition.

Summary

The unfilled 3*d* orbitals of Sc in its +3 oxidation state lead to semiconducting behaviour and improved phase stability for ScGaN and ScAlN alloys compared to all other TMN-AlN alloys. The epitaxial strain introduced in ScGaN/GaN, ScAlN/GaN and ScAlN/GaN device heterostructures enhances the alloy phase stability and allows the use of InGaN. The critical thicknesses for epilayer strain relaxation in these systems remain high enough to enable practical applications in optoelectronic and high-power electronic devices. The band gaps remain direct up to ~50% ScN in ScGaN and ~25% ScN in ScAlN. Carrier effective masses are high in wurtzite ScAlN, indicating low electron mobilities and a high probability of polaronic conduction. In contrast, electron mobilities in wurtzite ScGaN are expected to remain close to those of GaN, indicating better prospects for its use as an electronic material. ScGaN and ScAlN alloys with direct band gaps are also expected to have significantly higher exciton binding energies compared to GaN and AlN, while their enhanced piezoelectric coefficients indicate considerable promise for energy harvesting and high electron mobility transistor applications.

The remaining challenge for this material system is the growth of phase-pure, defect-free ScGaN alloys. Wurtzite-structure ScAlN films are free from stacking faults and zinc blende inclusions as the formation energy of the zinc blende phase is significantly higher for ScAlN than for ScGaN at low ScN contents. Epitaxial [0001]-oriented wurtzite-structure ScGaN films have been obtained on GaN but these films tend to contain basal plane stacking faults and are affected by the nucleation and growth of the zinc blende phase. One possible route to increase the stability of the wurtzite phase is the use of doping. Basal plane stacking fault densities in wurtzite-structure GaN can be reduced dramatically using Si-doping [92], while Si-doping has been shown to increase TM solubility limits in GaN [93] and co-doping with other transition metals (e.g. [30]) may promote the relative stability of the wurtzite phase. A ferroelectric nonpolar phase, predicted to appear for ScGaN at higher ScN contents near the wurtzite-rock salt phase transition, might also be stabilised using epitaxial 'templating' [52]. Therefore, the future remains bright regarding this promising new family of electronic materials.

Acknowledgements

MAM would like to acknowledge support from the Royal Society via a University Research Fellowship, from the EPSRC through grant EP/I036052/1 and from the ERC through the Starting Grant 'SCOPE'.

Notes and references

[a] Dept. Materials, Imperial College London, Exhibition Road, London SW7 2AZ, UK.
[b] Dept. Materials Science & Metallurgy, University of Cambridge, 27 Charles Babbage Road, Cambridge, CB3 0FS, UK.

† It's important that the *c/a* lattice parameter ratio and *u* values are relaxed fully as Sc introduces a local distortion [52, 68]. Calculations omitting this relaxation step may produce incorrect phase stability results.

†† Except for FeAlN in this study, possibly due to the influence of magnetic effects which were not the focus of these calculations.

1 J. Wu, *J. Appl. Phys.*, 2009, **106**, 011101
2 D Zhu. D. J. Wallis and C.J. Humphreys, *Rep. Prog. Phys.*, 2013, **76**, 106501
3 M. Kneissl, T. Kolbe, C. Chua, V. Kueller, N. Lobo, J. Stellmach, A. Knauer, H. Rodriguez, S. Einfeldt, Z. Yang, N.M. Johnson and M. Weyers, *Semicond. Sci. Technol.*, 2011, **26**, 014036
4 T. Palacios, A. Chakraborty, S. Rajan, C. Poblenz, S. Keller, S. P. DenBaars, J. S. Speck and U. K. Mishra, *IEEE Electron Device Letters*, 2007, **26**, 781
5 G. Piazza, V. Felmetsger, P. Muralt, R. H. Olsson and R. Ruby, *MRS Bulletin*, 2012, **37**, 1051
6 J. Zhang, H. Tong, G. Liu, J. A. Herbsommer, G. S. Huang and N. Tansu, *J. Appl. Phys.*, 2011, **109**, 053706
7 B. N. Pantha, I.-W. Feng, K. Aryal, J. Li, J.-Y. Lin and H.-X. Jiang, *Appl. Phys. Exp.*, 2011, **4**, 051001
8 D.A.B. Miller, D.S. Chemla, T.C. Damen, A.C. Gossard, W. Wiegmann, T.H. Wood, C.A. Burrus, *Phys. Rev. B.*, 1985, **32**, 1043
9 S. F. Chichibu, A. C. Abare, M. S. Minsky, S. Keller, S. B. Fleischer, J. E. Bowers, E. Hu, U. K. Mishra, L. A. Coldren, S. P. DenBaars and T. Sota, *Appl. Phys. Lett.*, 1998, **73**, 2006
10 D. F. Feezell, J. S. Speck, S. P. DenBaars, and S. Nakamura, *J. Display Technol.*, 2013, **9**, 190
11 H. Zhao, G. Liu, J. Zhang, J. D. Poplawsky, V. Dierolf, and N. Tansu, *Optics Express*, 2011, **19**, A991
12 M. F. Schubert, J. Xu, J. K. Kim, E. F. Schubert, M. H. Kim, S. Yoon, S. M. Lee, C. Sone, T. Sakong and Y. Parket, *Appl. Phys. Lett.*, 2008, **93**, 041102
13 H. Zhao, G. Liu, R. A. Arif and N. Tansu, *Solid-State Electronics,* 2010, **54**, 1119
14 S. Choi, M.-H. Ji, J. Kim, H. Jin Kim, M. M. Satter, P. D. Yoder, J.-H. Ryou, R. D. Dupuis, A. M. Fischer and F. A. Ponce, *Appl. Phys. Lett.*, 2012, **101**, 161110
15 Y-K. Ee, X-H. Li, J. Biser, W. Cao, H. M. Chan, R. P. Vinci, and N. Tansu, *IEEE J. Sel. Top. Quantum Electron.*, 2009, **15**, 1066
16 Y. Li, S. You, M. Zhu, L. Zhao, W. Hou, T. Detchprohm, Y. Taniguchi, N. Tamura, S. Tanaka, and C. Wetzel, *Appl. Phys. Lett.* 2011, **98**, 151102
17 T. Markurt, L. Lymperakis, J. Neugebauer, P. Drechsel, P. Stauss, T. Schulz, T. Remmele, V. Grillo, E. Rotunno, and M. Albrecht, *Phys. Rev. Lett.* 2013, **110**, 036103
18 S. Nakamura, *Science*, 1998, **281**, 956
19 M. S. Ferdous, X. Wang, M. N. Fairchild, and S. D. Hersee, *Appl. Phys. Lett.*, 2007, **91**, 231107

Journal of Materials Chemistry A Accepted Manuscript

20 S. Kamiyama, M. Iwaya, S. Takanami, S. Terao, A. Miyazaki, H. Amano and I. Akasaki, *Physica Status Solidi A*, 2002, **192**, 296
21 Z. Bougrioua M. Azize, P. Lorenzini, M. Laügt and H. Haas, *Physica Status Solidi A*, 2005, **202**, 536
22 O. Igarashi, *Jpn. J. Appl. Phys.*, 1988, **27**, 790
23 S. Kerdsongpanya, B. Alling and P. Eklund, *J. Appl. Phys.*, 2013, **114**, 073512
24 S. Kerdsongpanya, B. Alling, and P. Eklund, *Phys. Rev. B*, 2012, **86**, 195140
25 P. V. Burmistrova, J. Maassen, T. Favaloro, B. Saha, S. Salamat, Y. R. Koh, M. S. Lundstrom, A. Shakouri and T. D. Sands, *J. Appl. Phys.*, 2013, **113**, 153704
26 B. Saha, J. Acharya, T. D. Sands, and U. V. Waghmare, *J. Appl. Phys.*, 2010, **107**, 033715
27 H. Lind, F Tasnadi and I A Abrikosov, *New J. Phys.*, 2013, **15**, 095010
28 A. Bonanni, *Semicond. Sci. Technol.*, 2007, 22, R41
29 D. Holec, R. Franz, P. H. Mayrhofer and C. Mitterer, *J. Phys. D: Appl. Phys.*, 2010, **43**, 145403
30 D. Holec, L. Zhou, R. Rachbauer, and P. H. Mayrhofer, *J. Appl. Phys.*, 2013, **113**, 113510
31 A. Bonanni, M. Kiecana, C. Simbrunner, T. Li, M. Sawicki, M. Wegscheider, M. Quast, H. Przybylińska, A. Navarro-Quezada, R. Jakieła, A. Wolos, W. Jantsch, and T. Dietl, *Phys. Rev. B*, 2007, **75**, 125210
32 E. Sarigiannidou, F. Wilhelm, E. G. R. Monroy, E. Bellet-Amalric, A. Rogalev, J. Goulon, J. Cibert and H. Mariette *Phys. Rev. B*, 2006, **74**, 041306
33 A. Y. Polyakov, N. B. Smirnov, A. V. Govorkov, R. M. Frazier, J. Y. Liefer, G. T. Thaler, C. R. Abernathy, S. J. Pearton, and J. M. Zavada, *Appl. Phys. Lett.*, 2004, **85**, 4067
34 R. Frazier, G. Thaler, M. Overberg, B. Gila, C. Abernathy and S. Pearton, *Appl. Phys. Lett.*, 2003, **83**, 1758
35 K. Y. Ko, Z. H. Barber and M. G. Blamire, *J. Appl. Phys.*, 2006, **100**, 083905
36 D. Pan, J. K. Jian, A. Ablat, J. Li, Y. F. Sun and R. Wu, *J. Appl. Phys.*, 2012, **112**, 053911
37 F. A. Cotton and G. Wilkinson, *Advanced Inorganic Chemistry*, 5th Edn. Wiley-Blackwell, 1988
38 D. Gall, I. Petrov and J. E. Greene, *J. Appl. Phys.*, 2001, **89**, 401
39 W.R. Lambrecht, *Phys. Rev. B.*, 2000, 62, 13538
40 D. Gall, M. Stadele, K. Jarrendahl, I. Petrov, P. Desjardins, R. T. Haasch, T.-Y. Lee and J. E. Greene, *Phys. Rev. B.*, 2001, **63**, 125119
41 X. Bai, Ph. D. thesis, Ohio University, Athens, Ohio 2000.
42 M.A. Moram, Z.H. Barber and C.J. Humphreys, *Thin Solid Films*, 2008, **516**, 8569
43 M. A. Moram, Y. Zhang, M. J. Kappers, Z. H. Barber, and C. J. Humphreys, *Appl. Phys. Lett.*, 2007, **91**, 152101
44 J. M. Gregoire, S. D. Kirby, G. E. Scopelianos, F. H. Lee, and R. B. van Dover, *Phys. Rev. B*, 2008, **104**, 074913
45 J. P. Dismukes, W. M. Yim, J. J. Tietjen, and R. E. Novak, *RCA Review*, 1970, **31**, 680
46 D. Gall, I. Petrov, N. Hellgren, L. Hultman, J. E. Sundgren, and J. E. Greene, *J. Appl. Phys.*, 1998, **84**, 6034
47 H. Al-Brithen and A. R. Smith, *Appl. Phys. Lett.*, 2000, **77**, 2485
48 A. R. Smith, H. A. H. Al-Brithen, D. C. Ingram and D. Gall, *J. Appl. Phys.*, 2001, **90**, 1809
49 J.H. Edgar, T. Bohnen and P.R. Hageman, *J. Cryst. Growth*, 2008, **310**, 1075
50 M.A. Moram, S.V. Novikov, A.J. Kent, C. Norenberg, C.T. Foxon and C.J. Humphreys, *J. Cryst. Growth*, 2008, **310**, 2746
51 M. A. Moram, Z. H. Barber, C. J. Humphreys, T. B. Joyce and P. R. Chalker, *J. Appl. Phys.*, 2006, **100**, 023514
52 S. Zhang, D. Holec, C.J. Humphreys and M.A. Moram, *J. Appl. Phys.*, 2013, **114** , 133510
53 P.H. Mayrhofer, D. Music and J.M. Schneider, *J. Appl. Phys.*, 2006, **100**, 094906
54 P. Mayrhofer, D. Music, T. Reeswinkel, H.-G. Fuß and J. Schneider, *Acta Mater.*, 2008, **56**, 2469
55 N.B. Sedrine, A. Zukauskaite, J. Birch, L. Hultman and V. Darakchieva, *Jap. J. Appl. Phys.*, 2013, **52**, 08JM02
56 P. H. Mayrhofer, D. Music, and J. M. Schneider, *Appl. Phys. Lett.*, 2006, **88**, 071922
57 I. H. Ho and G. B. Stringfellow, *Appl. Phys. Lett.*, 1996, **69**, 2701
58 M. Akiyama, K. Kano and A. Teshigahara, *Appl. Phys. Lett.*, 2009, **95**, 162107
59 C. Höglund, J. Bareño, J. Birch, B. Alling, Z. Czigány and L. Hultman, *J. Appl. Phys.*, 2010, **105**, 113507
60 R. Deng, S. R. Evans and D. Gall, *Appl. Phys. Lett.*, 2013, 102, 112103
61 C. Höglund, J. Birch, B. Alling, J. Bareño, Z. Czigány, P. O. Å. Persson, G. Wingqvist, A. Zukauskaite and L. Hultman, *J. Appl. Phys.*, 2010, **107**, 123515; B. Alling, A. Karimi, and I. Abrikosov, *Surf. Coat. Technol.*, 2008, **203**, 883
62 M. Akiyama, T. Kamohara, K. Kano, A. Teshigahara, Y. Takeuchi and N. Kawahara, *Adv. Mater.*, 2009, **21**, 593
63 G. Wingqvist, F. Tasnadi, A. Zukauskaite, J. Birch, H. Arwin and L. Hultman, *Appl. Phys. Lett.*, 2010, **97**, 112902
64 A. Zukauskaite, G. Wingqvist, J. Palisaitis, J. Jensen, P.O.A. Persson, R. Matloub, P. Muralt, Y. Kim, J. Birch and L. Hultman, *J. Appl. Phys.*, 2012, **111**, 093527
65 T. Bohnen, G.R. Yazdi, R. Yakimova, G.W.G. van Dreumel, P.R. Hageman, E. Vlieg, R.E. Algra, M.A. Verheijen and J.H. Edgar, *J. Cryst. Growth*, 2009, **311**, 3147
66 W. W. Lei, D. Liu, P. W. Zhu, X. H. Chen, Q. Zhao, G. H. Wen, Q. L. Cui, and G. T. Zou, *Appl. Phys. Lett.*, 2009, **95**, 162501
67 C. Constantin, H. Al-Brithen, M. B. Haider, D. Ingram and A. R. Smith, *Phys. Rev. B*, 2004, **70**, 193309
68 C. Constantin, M. B. Haider, D. Ingram, A. R. Smith, N. Sandler, K. Sun and P. Ordejón, *J. Appl. Phys.*, 2005, **98**, 123501
69 M. E. Little and M. E. Kordesch, *Appl. Phys. Lett.*, 2001, **78**, 2891
70 D. Holec, F. Rovere, P. H. Mayrhofer and P. B. Barna, *Scripta Mater.*, 2010, **62**, 349
71 M.A. Moram, Y. Zhang, T.B. Joyce, D. Holec, P.R. Chalker, P.H. Mayrhofer, M.J. Kappers and C.J. Humphreys, *J. Appl. Phys.*, 2009, **106**, 113533
72 S.M. Knoll, S. Zhang, T.B. Joyce, M.J. Kappers, C.J. Humphreys and M.A. Moram, *Physica Status Solidi A* , 2012, **209**, 33
73 S. Y. Karpov, *MRS Internet J. Nitride Semicond. Res.*, 1998, **3**, 16
74 J. Z. Liu and A. Zunger, *Phys. Rev. B*, 2008, **77**, 205201

Journal of Materials Chemistry A Accepted Manuscript

This journal is © The Royal Society of Chemistry 2012

75 C. Höglund, B. Alling, J. Birch, M. Beckers, P. O. Å. Persson, C. Baehtz, Z. Czigány, J. Jensen and L. Hultman, *Phys. Rev. B*, 2010, **81**, 224101
76 A. Šimůnek, J. Vackář and K. Kunc, *Phys. Rev. B.*, 2005, **72**, 045110
77 V. Ranjan, L. Bellaiche and E. J. Walter, *Phys. Rev. Lett.*, 2003, **90**, 257602
78 N. Farrer and L. Bellaiche, *Phys. Rev. B*, 2002, 66, 201203R
79 S. Zhang, W. Y. Fu, D. Holec, C. J. Humphreys and M. A. Moram, *J. Appl. Phys.* 2014, DOI: 10.1063/1.4848036
80 M.G. Moreno-Armenta, L. Mancera and N. Takeuchi, *Physica Status Solidi B*, 2003, 238, 127
81 I. Vurgaftman and J. R. Meyer, *J. Appl. Phys.*, 2003, **94**, 3675
82 K. Shimada, M. Takouda, Y. Hashiguchi, S. F. Chichibu, M. Hata, H. Sazawa, T. Takada and T. Sota, *Semicond. Sci. Technol.*, 2012, **27**, 105014
83 V. Petrman and J. Houska, *J. Mater. Sci.*, 2013, **48**, 7642
84 D. Holec, M. Friak, J. Neugebauer and P. H. Mayrhofer, *Phys. Rev. B.*, 2012, **85**, 064101
85 M. A. Moram and M. E. Vickers, *Rep. Prog. Phys.*, 2009, 72, 036502
86 F. Tasnádi, B. Alling, C. Höglund, G. Wingqvist, J. Birch, L. Hultman, and I. A. Abrikosov, *Phys. Rev. Lett.*, 2010, **104**, 137601
87 H. Liu, F. Zeng, G. Tang and F. Pan, *Appl. Surf. Sci.*, 2013, **270**, 225
88 R. Matloub, A. Artieda, C. Sandu, E. Milyutin and P. Muralt, *Appl. Phys. Lett.*, 2011, **99**, 092903
89 M. Moreira, J. Bjurström, I. Katardjev and V. Yantchev, *Vacuum*, 2011, **86**, 23
90 P. H. Mayrhofer, F. D. Fischer, H. J. Bohm, C. Mitterer and J. M. Schneider, *Acta Mater.*, 2007, **55**, 1441
91 N. Takeuchi, *Phys. Rev. B*, 2002, **65**, 045204
92 M. Wieneke, M. Noltemeyer, B. Bastek, A. Rohrbeck, H. Witte, P. Veit, J. Bläsing, A. Dadgar, J. Christen and A. Krost, *Physica Status Solidi B*, 2010, **248**, 578
93 A. Bonanni, A. Navarro-Quezada, Tian Li, M. Wegscheider, Z. Mate, V. Holy, R.T. Lechner, G. Bauer, M. Rovezzi, F. D'Acapito, M. Kiecana, M. Sawicki and T. Dietl, *Phys. Rev. Lett.*, 2008, **101**, 135502

Journal of Materials Chemistry A Accepted Manuscript